

Landslides (2007) 4:43–51
 DOI 10.1007/s10346-006-0051-2
 Received: 10 August 2005
 Accepted: 14 July 2006
 Published online: 6 September 2006
 © Springer-Verlag 2006

Ogbonnaya Igwe · Kyoji Sassa · Fawu Wang

The influence of grading on the shear strength of loose sands in stress-controlled ring shear tests

Abstract Three silica sand samples—well graded, intermediately graded, and narrowly graded—having different uniformity coefficients, were constituted to allow the investigation of the influence of particle size distribution on their mechanical behavior. Using a ring shear apparatus, samples were tested under a wide range of laboratory conditions. Results of the tests clearly indicate that, for specimens confined under identical stress conditions, well-graded specimens have higher values of peak and steady state strengths than the rest of the specimens. A relationship between uniformity coefficient and shear strengths shows that the higher the uniformity coefficient, the higher the shear strength. On account of these, well-graded specimens have higher static liquefaction resistance than the poorly graded specimens. Within the range of normal stresses employed in the tests, results reveal that not only are poorly graded sands more likely to suffer higher postfailure strength reduction, but that their steady-state strengths are easily reduced to zero, the magnitude of the confining stress notwithstanding. This reduction of shear resistance to zero has been described as complete liquefaction in this paper. While almost all of the narrowly graded specimens suffered complete liquefaction, widely graded ones did not; an observation that seem to highlight the influence of grading on the mechanical behavior of the sands.

Keywords Narrowly graded specimens · Intermediately graded specimens · Well-graded specimens

Introduction

Assessment of the liquefaction potential of sands when selecting them for civil engineering works is of immense importance in the construction industry. Because a great deal of failures of earth structures, foundations, and slopes founded on sands have been attributed to the liquefaction of the sands, stakeholders in environmental protection and urban development have elevated the importance of liquefaction-evaluation by placing it at the heart of their management policies. This has inspired intense research. Classic examples have led to, for instance, better knowledge of the factors and dynamics behind the failure of Fort Peck Dam in Montana in 1938 (Finn et al. 1970; Newmark and Rosenblueth 1971); Calaveras Dam in California in 1920 (Hardin and Drenevich 1972a,b); the Lower Lan Norman Dam (Pyke 1973); the foundation failures induced by the 1964 earthquake in Alaska, USA, and Niigata, Japan (Herrera 1964); and the flow slides in the province of Zealand in Holland (Hardin and Drenevich 1972a,b; Kondner and Zelasko 1963) and Mississippi River (Seed and Idriss 1971). Although some of these failures were triggered by earthquake shaking and others by monotonic loading, one salient fact emerging from field and laboratory investigations is that the sands responsible for the failures would all be regarded as loose in any kind of classification system—whether based on blowcounts, Dutch cone penetration, or relative density (Castro and Poulos 1977). In response, researchers have undertaken extensive cyclic

and monotonic tests, performing experiments on loose, saturated sands to unravel the mechanism underlying the readiness of the sands to liquefy. Liquefaction of saturated sands, often regarded as the fundamental cause of flow slides, has been responsible for many of the tragedies resulting from slope failures. Many have postulated that the breakdown of a metastable structure in loose soils in association with excessive volume changes during loading ultimately leads to collapse and liquefaction. Important works by Castro (1969), Casagrande (1936, 1976), Seed and Idriss (1969), Bishop (1971, 1973), Castro and Poulos (1977), Poulos, (1981), Poulos et al. (1985), Sladen et al. (1985), Vaid and Chern, (1985); Alarcon-Guzman et al. (1988), Negussey et al. (1988), Kramer and Seed (1988), Vasquez-Herrera et al. (1988), Konrad (1993), Sasitharan et al. (1993), Sasitharan et al. (1994), Lade and Pradel (1990), Sassa (1985, 2000), Sassa et al. (2003), and Wang and Sassa (2002) bear witness to the extent of research and interest in soil liquefaction.

However, in spite of the enormous amount of work done so far, not much is known about the influence of particle gradation on the liquefaction potential of loose sands, especially when the sands are subject to long shear displacements in the ring shear apparatus. Understanding the relationship between the rapid reduction in strength and catastrophic landslides, and clarifying the influence of gradation on both postfailure mobility and the steady state strength of sands sheared under undrained conditions would require ring shear tests, where specimens could be displaced for long distances.

Overview of recent research

Although many published works exist, some of them predating Hutchinson and Townsend (1961), scarcity of conclusive laboratory evidences, irregularities arising from design of laboratory apparatus, narrow range of materials investigated, and, sometimes, difficulty in distinguishing the effects of particle gradation from those of particle size, have combined to limit what is presently known on the subject. In spite of this, however, there is evidence that relates liquefaction potential with gradation.

Vaid et al. (1990), in their well-known publication on particle gradation and liquefaction, studied the resistance to liquefaction of three medium sands having linear grain-size distribution curves, identical mean grain size and mineralogy, but different uniformity coefficients—1.5, 3.0, and 6.0. They found that at low relative densities, poorly graded, water-placed sand had lower cyclic strength than the well-graded (WG) sands at the same relative density. Interestingly, they found that the reverse trend was true at higher relative densities. At higher relative densities, the poorly graded, water-placed sands had higher cyclic strength than the WG ones. They observed, in addition, that within a certain range of relative densities—from the loosest state to a relative density of about 43%—the poorly graded sands deformed in a contractive manner, whereas the WG ones, within the same range of relative densities, did not. They concluded, on this evidence, that gradation

might control the occurrence of contractive behavior, and possibly, flow failure at low relative densities.

Some recent effort by Kokusho et al. (2004) has shown that, unless a WG sample is composed of easily crushable or strongly weathered particles, it has undrained monotonic strength considerably higher than that of a poorly graded one. Laboratory tests on poorly graded soils by several researchers, including Sasitharan et al. (1993), Yamamuro and Lade (1999), Yoshimine et al. (1999), and Wang and Sassa (2001, 2002), indicate that poorly graded soils have low liquefaction resistance. But, while the low peak strengths of poorly graded sands, often cited as evidence of high liquefaction potential, are significantly understood, neither the steady-state strengths nor the postliquefaction deformation characteristics of these sands, especially when they are subjected to large shear displacements, has been properly understood. This is where the ring shear apparatus, which permits unlimited shearing displacements of soils, becomes important. Our paper attempts to investigate the influence of gradation on both the pre- and postliquefaction strengths of loose silica sands and to examine their postfailure deformation behavior using a ring shear apparatus that is capable of precise measurements of shear resistance and excess pore pressure while also permitting specimens to undergo large shear displacements.

Testing program

Apparatus

The results presented and discussed in this paper are from a ring shear apparatus, hereafter referred to as DPRI-5, which is the fifth version of ring shear apparatus available at the Disaster Prevention Research Institute, Kyoto University, Japan. Designed, modified, and vastly improved by Sassa in 1996, DPRI-5 is equipped with devices capable of sustaining undrained loading throughout the duration of a test. The apparatus is designed to eliminate some difficulties commonly encountered while studying the mechanism of landslide motion and is sufficiently equipped to allow speed- and stress-controlled tests and the measurement of very large shear displacement. Details of the design and efficiency of the apparatus have been discussed comprehensively by Sassa et al. (2003) and Wang and Sassa (2001).

Specimen characteristics

Industrial sand materials composed of subangular to angular quartz and small amounts of feldspar were reconstituted to three uniformity coefficients—3.3, 4.5, and 9.0—referred to as narrowly graded (NAG), intermediately graded (ING), and WG. The grain size distribution curves are shown in Fig. 1, while the physical properties of the samples are summarized in Table 1. Angularity and mineral composition was uniform among the different size fractions.

Sample preparation and testing procedure

Oven-dried specimens with the desired uniformity coefficients were placed in the shear box by moist tamping method. Thereafter, test specimens were saturated with water. To achieve B_D of at least 0.95 saturation, which was the minimum acceptable value used in this study, carbon dioxide was first introduced into the samples, at a slow rate, for at least 1 h, after which, deaired water was introduced, again at a slow rate, to ensure adequate saturation. B_D parameter—the ratio of change in pore pressure and change in

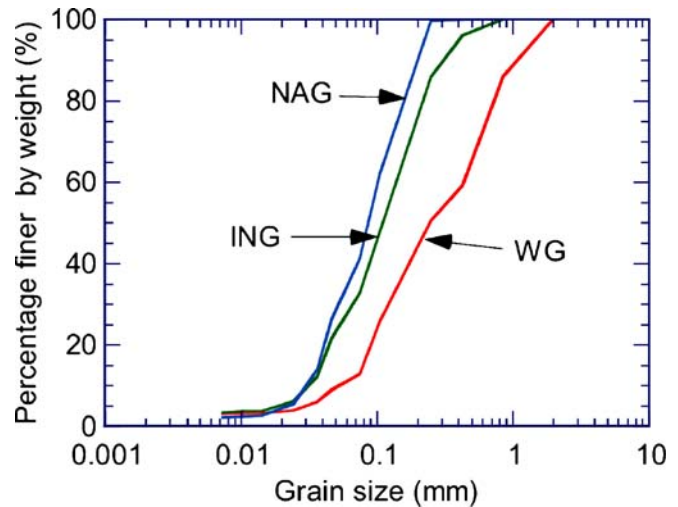


Fig. 1 Grain size distribution curves

normal stress ($\Delta u/\Delta\sigma$) over a specified period of time—was the standard parameter used in assessing the degree of saturation of the test samples (Sassa 1988).

Obtaining the B_D parameter involved a simple process of consolidating the samples at 49 kPa normal stress in drained condition, and increasing the normal stress to 98 kPa in undrained condition when a constant value of vertical displacement signaled the end of the consolidation process, which lasted an average of 60 min. The resultant increase in pore pressure (from zero to a certain monitored value), Δu , divided by the corresponding increase in normal stress (from 49 to 98 kPa), $\Delta\sigma$, is the B_D parameter. Specimens were considered fully saturated if the B_D was equal to or greater than 0.95. The objectives of the present research did not permit the overconsolidation of specimens. In light of this, all samples were normally consolidated, and thereafter, shearing was performed by incremental increase of shear stress at the rate of 0.98 kPa/s.

Test results

Narrowly graded specimens

A summary of the results is presented in Table 2. Test result (no. 1) of a NAG specimen with a relative density of 33.1%, shown in Fig. 2, presents the mechanism of liquefaction and flow failure in granular materials. Its behavior tends to replicate the mobility and state of liquefied materials in the field. They do not only have intense mobility; they also possess low peak and steady state strengths. It is clear that soon after reaching a peak resistance of 49 kPa at just 1.1 mm, it underwent rapid loss of strength that saw its resistance decrease to about 7 kPa at steady state (Fig. 2b). It is noted that

Table 1 Physical properties of the materials

Specimen	Minimum dry density (g/cm^3)	Maximum dry density (g/cm^3)	Mean grain size (D_{50})	Effective grain size (D_{10})	Uniformity coefficient (Uc)	Specific gravity
WG	1.38	1.82	0.23	0.04	9.0	2.65
ING	1.26	1.68	0.11	0.03	4.5	2.65
NAG	1.24	1.66	0.08	0.03	3.3	2.65

Table 2 Summary of test results on relative density, normal stress, peak strength, and steady-state strength

Test no.	Sample	Condition	Relative density (%)	Normal stress (kPa)	Peak strength (kPa)	Steady-state strength (kPa)	Figure no.
1	NAG	Undrained	33.1	201	49	7	Fig. 2
2	NAG	Drained	32.1	200	142	136	Fig. 3
3	NAG	Undrained	29.5	220	49	0	Fig. 4
4	NAG	Undrained	29.5	305	85	0	Fig. 5
5	NAG	Undrained	29.4	257	70	0	Fig. 6
6	ING	Undrained	29.2	202	54	5	Fig. 7
7	ING	Drained	29.4	196	128	122	Fig. 8
8	ING	Undrained	29.1	262	67	0	Fig. 9
9	ING	Undrained	31.5	290	97	10	Fig. 10
10	WG	Undrained	29.5	196	60	12	Fig. 11
11	WG	Undrained	29.5	250	80	13	Fig. 12
12	WG	Undrained	29.5	290	106	12	Fig. 13
13	WG	Drained	30.2	196	146	137	Fig. 14

within the period under consideration, the fast drop in shear resistance corresponded to the rapid increase in excess pore water pressure (Fig. 2c). It might be important to note that, while the specimen mobilized its peak at about 1.6 mm shear displacement, it attained its steady state strength of about 7 kPa at around 62 mm shear displacement (Fig. 2b).

A drained test was undertaken to investigate the nature of volume changes associated with loose NAG samples. Close examination of the result of drained test (Fig. 3) of a specimen consolidated at 200 kPa to $Dr=32.2\%$ shows that, soon after shearing commenced, the specimen first suffered considerable volume reduction until around 30 mm, from which point the sample underwent less volume reduction until the test was terminated at 10 m. The cause of volume reduction is considered to be the collapse of the metastable structure and grain crushing within the shear zone after its formation. Volume reduction before the peak (point P in Fig. 3) where the sliding surface is formed (Wafid et al. 2004) was caused by the collapse of the metastable structure. The major cause of volume reduction after the peak is considered to be grain crushing along the sliding surface, especially after a certain shearing point (point M in Fig. 3), when the effect of collapse no longer exists. This result, while highlighting the importance of ring shear tests in understanding the behavior of soils sheared to long distances, clearly shows that grain crushing is a central factor in postfailure mobility of even loose sands.

While the rapid decrease of shear resistance after attaining peak strength, observed in the specimens in which liquefaction developed, has been widely recognized and published in studies using triaxial tests, the present study attempts to highlight some new ideas by showing that gradation not only affects peak strengths but exerts a strong influence on the postfailure behavior and strengths of loose sands sheared for long distances.

The result of a very loose and fully saturated specimen subjected to an undrained ring shear test is shown in Fig. 4. It demonstrates that not only does a NAG specimen, whose relative density is looser than about 30%, instantly liquefies when stressed, but that it achieves a very low steady state strength, close to zero. The entire behavior leading to negligible steady state strength has been termed complete liquefaction in this paper. Figure 4 shows that the sample was consolidated at 220 kPa to a relative density of

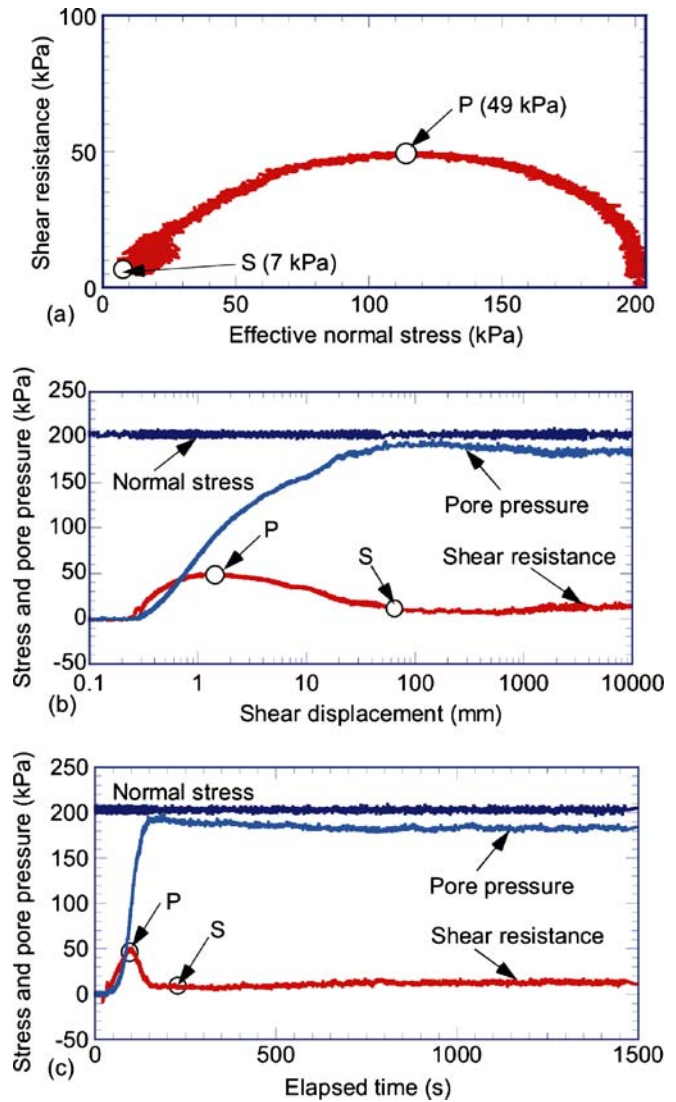


Fig. 2 Undrained response of NAG specimen (test 1) with $Dr=33.1\%$, $\sigma'_c=201$ kPa, $B_D=0.97$. **a** Stress path; **b** stress and pore pressure vs displacement; **c** vs elapsed time

29.5%. It may be seen that, soon after reaching a peak resistance of 49 kPa at 1.6 mm (point marked P), it underwent rapid loss of strength that saw its resistance decrease to near zero (point marked S),

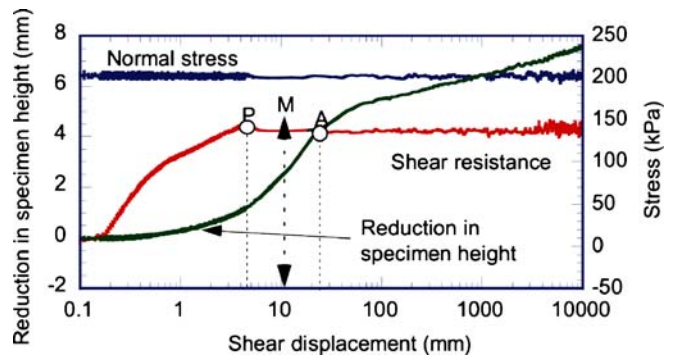


Fig. 3 Drained response of NAG specimen (test 2) with $Dr=32.2\%$; $\sigma'_c=200$ kPa; $B_D=0.97$

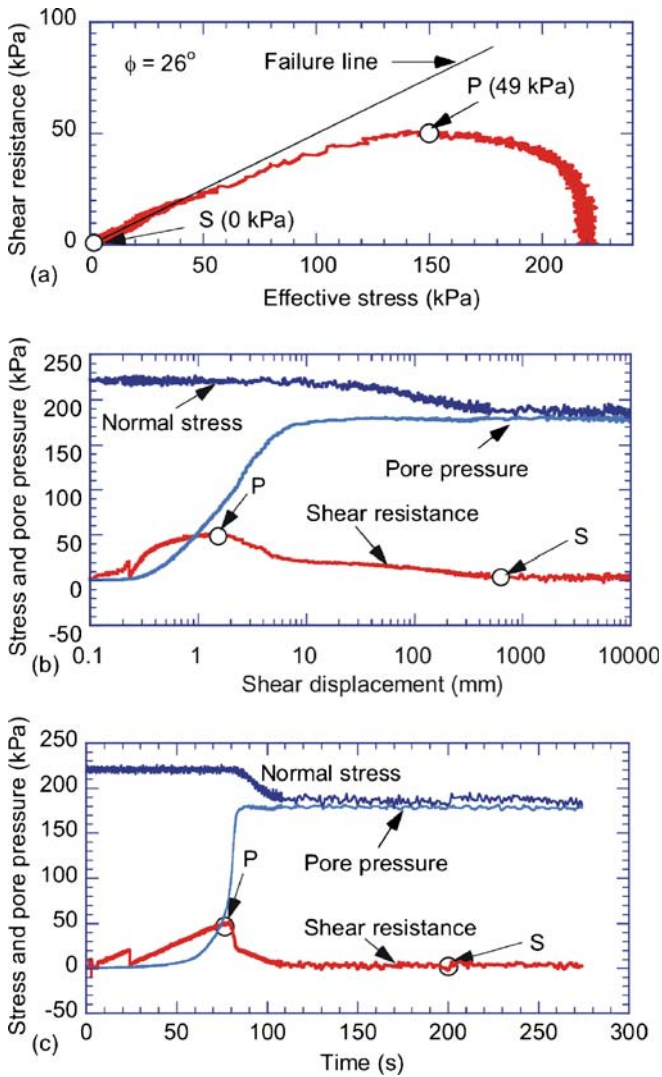


Fig. 4 Undrained shear behavior of NAG specimen (test 3) $D_r=29.5\%$, $\sigma'_c=220$ kPa, $B_D=0.97$. **a** Stress path; **b** shear resistance, normal stress, and pore pressure vs displacement

and it remained so until shearing was terminated at 10 m shear displacement.

The specimen acquired a brittleness index of 1.0 during the process. Similarly, another NAG specimen (Fig. 5), consolidated at 305 kPa to a relative density of 29.5%, liquefied and acquired a high brittleness index of 0.96. Careful observation confirms that, although the specimen attained a peak strength of 85 kPa (point marked P), it suffered substantial loss of strength soon after attaining this peak until it reached negligible steady-state strength. Yet another specimen (Fig. 6) consolidated at 257 kPa to a relative density of 29.4% achieved peak strength of 70 kPa at about 1.6 mm, failed, and underwent quick reduction in its strength. By point S (Fig. 6b), corresponding to about 165 s (Fig. 6c), the resistance of the specimen had already reached zero and remained zero until the experiment was terminated after about 655 mm of displacement. The brittleness index was 1.0.

The behaviors of the specimens described above are not only indications of the readiness of the NAG specimens to undergo complete liquefaction failure but are also evidence that allowing

shear deformation to go on for long distances could clarify the influence of gradation on the postfailure behavior of granular materials.

Intermediately graded specimens

The mechanical behavior of an ING specimen when loaded undrained is presented in Fig. 7. The specimen was consolidated at 202 kPa to a relative density of 29.2%. It could be observed that after the sample reached its peak strength of 54 kPa at about 1 mm (point P in Fig. 7b), its shear resistance suffered severe and rapid reduction until the resistance became 5 kPa at around 10 mm (point S in Fig. 7) and remained so until the test was terminated at 1 m of shear displacement. This loss of shear resistance indicated a high brittleness index of 0.91. The corresponding pore pressure increase, within the period under consideration, may be mentioned. By 10-mm shear displacement, pore pressure had risen to a value as high as 187 kPa, which was about 93% of the normal stress.

A drained test on a specimen of ING consolidated at 196 kPa to a relative density of 29.4% showed that considerable re-

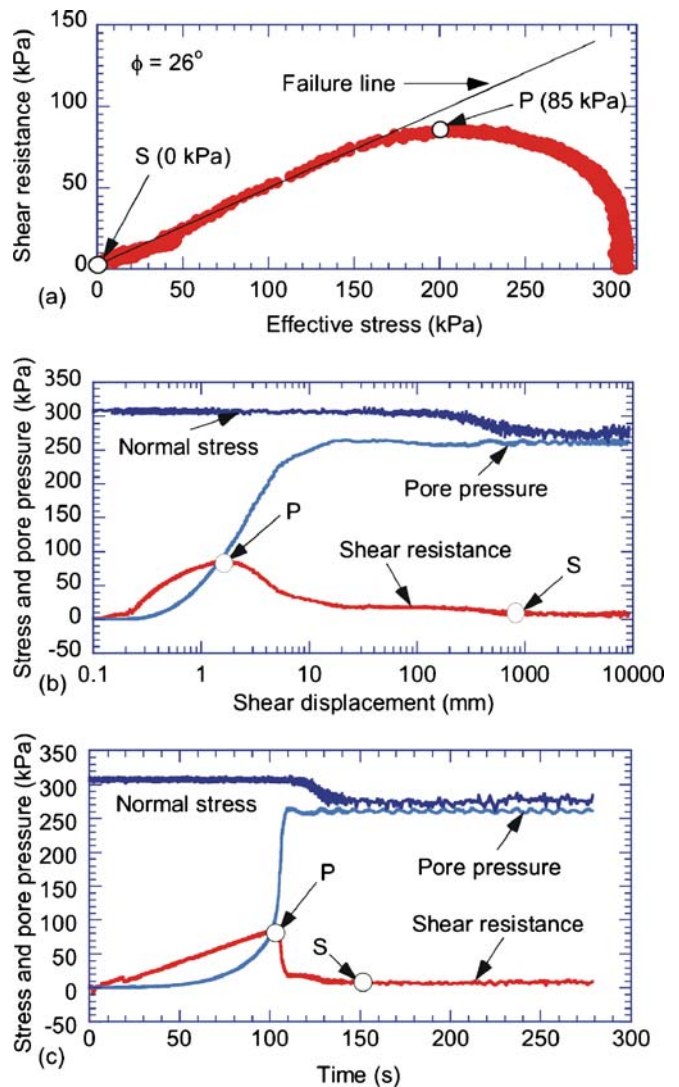


Fig. 5 Undrained response of NAG (test 4) specimens $D_r=29.5\%$, $\sigma'_c=305$ kPa, $B_D=0.96$. **a** Stress path; **b** shear resistance, normal stress, and pore pressure vs displacement; **c** vs elapsed time

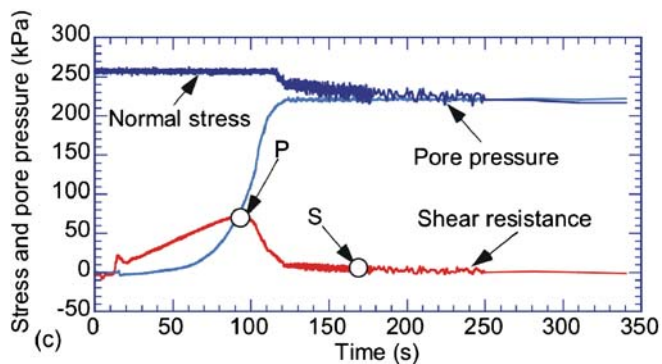
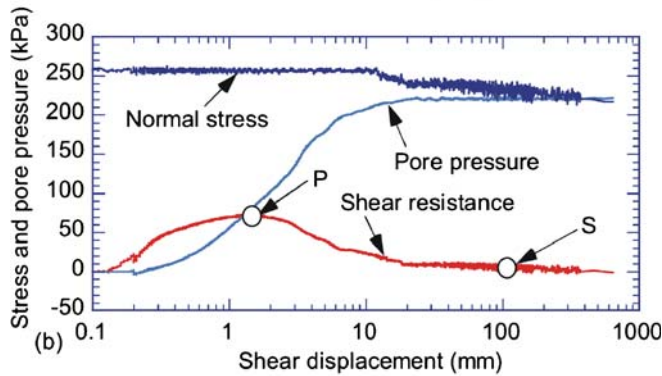
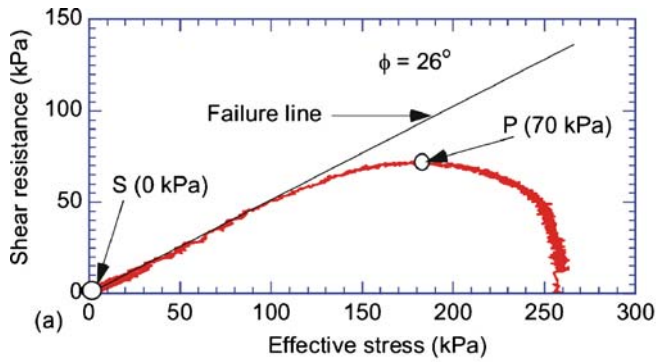


Fig. 6 Undrained response of NAG specimen (test 5) $D_r=29.4\%$, $\sigma'_c=257$ kPa, $B_p=0.96$. **a** Stress path; **b** shear resistance, normal stress, and pore pressure vs displacement; **c** vs elapsed time

duction in specimen height. But, unlike the trend of height reduction associated with the NAG specimen described in the previous section, the height reduction in the ING could be divided into two main phases, AB and BC, with the slope of BC close to 90° (Fig. 8). The first major postpeak volume reduction AB is much less than the volume reduction BC occurring between 129- and 237-mm shear displacement. While this result might suggest that a second and more significant volume reduction is possible towards the steady state, the exact cause of the factor responsible for this phenomenon is not well known at present. Further tests are required to understand whether or not this particular behavior may be linked to the transition from slide to flow phenomenon often cited as the mechanism of destructive flow slides.

Another specimen consolidated at about 262 kPa, and having a relative density of 29.1% (Fig. 9), seems to follow the same behavioral trend. The specimen attained its peak strength of 67 kPa at about 1.4 mm (point P in Fig. 9b). What followed was a fast

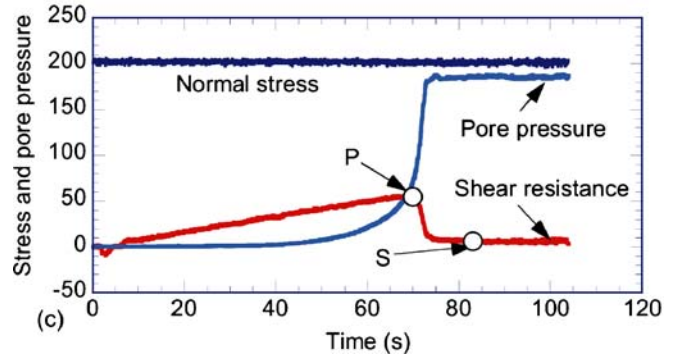
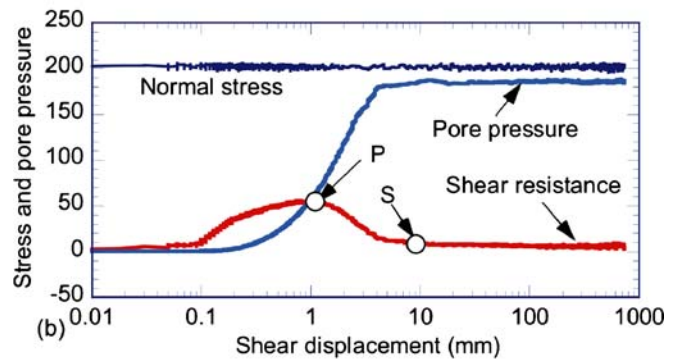
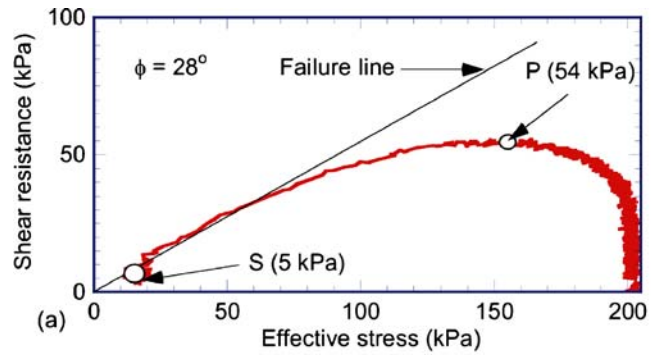


Fig. 7 Undrained response of ING specimen (test 6) $D_r=29.2\%$, $\sigma'_c=202$ kPa, $B_p=0.96$. **a** Stress path; **b** shear resistance, normal stress, and pore pressure vs displacement; **c** vs elapsed time

decrease in shear resistance until the shear resistance became zero and remained zero until the test was terminated after 10 m of shear displacement (Fig. 9b). The specimen had a brittleness index of 1.0

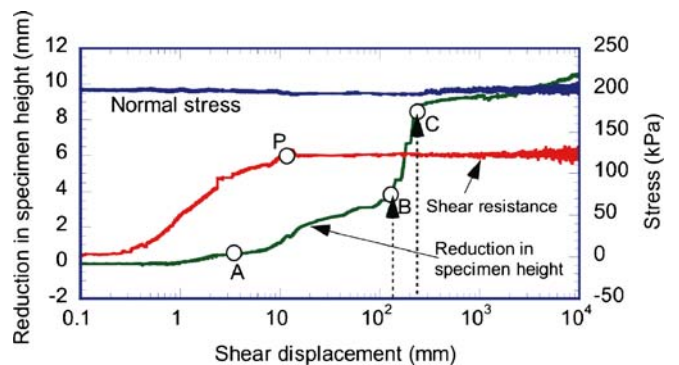


Fig. 8 Drained response of ING specimen (test 7) with $D_r=29.4\%$; $\sigma'_c=196$ kPa; $B_p=0.97$

as a result. Similarly, another specimen confined at about 290 kPa to a relative density of 31.5% (Fig. 10) shows that its resistance rose to a peak of 97 kPa at about 2 mm. Soon after, the specimen failed and suffered rapid reduction in shear resistance (Fig. 10c) until it attained a steady-state strength of 10 kPa. The brittleness index was about 0.90. It may be important to note that, by 23-mm (point W in Fig. 10b) shear displacement, the pore pressure had risen to a value of 250 kPa, ensuring a pore pressure ratio of about 0.88.

Well-graded specimens

Undrained shear behavior of a WG specimen in loose state is presented in Fig. 11. The specimen was consolidated at 196 kPa to a relative density of 29.5%. The stress path of the specimen is shown in Fig. 11a, while the shear resistance and pore pressure relationship with shear displacement is illustrated in Fig. 11b. It may be seen from Fig. 10a that after the material reached a peak shear strength of 60 kPa (point P), the sample appeared to have collapsed and underwent rapid loss of resistance until it attained its steady state strength of about 12 kPa (point S in Fig. 11). As a result, the

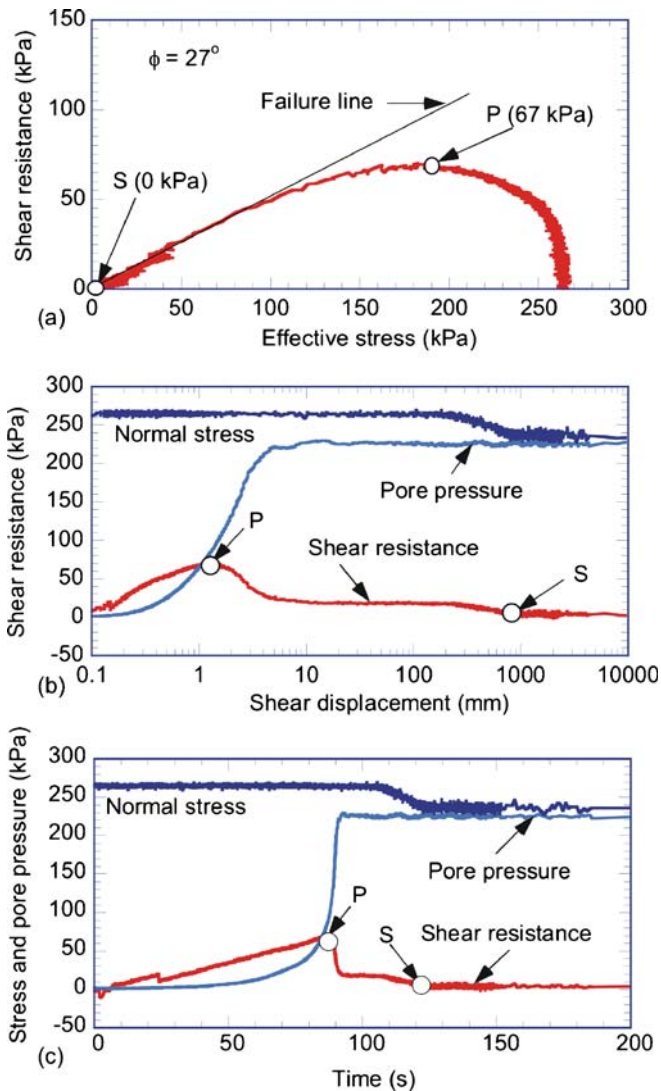


Fig. 9 Shear behavior of ING specimens (test 8) $D_r=29.1\%$, $\sigma_c=262$ kPa, $B_D=0.97$. **a** Stress path; **b** shear resistance, normal stress, and pore pressure vs displacement; **c** vs elapsed time

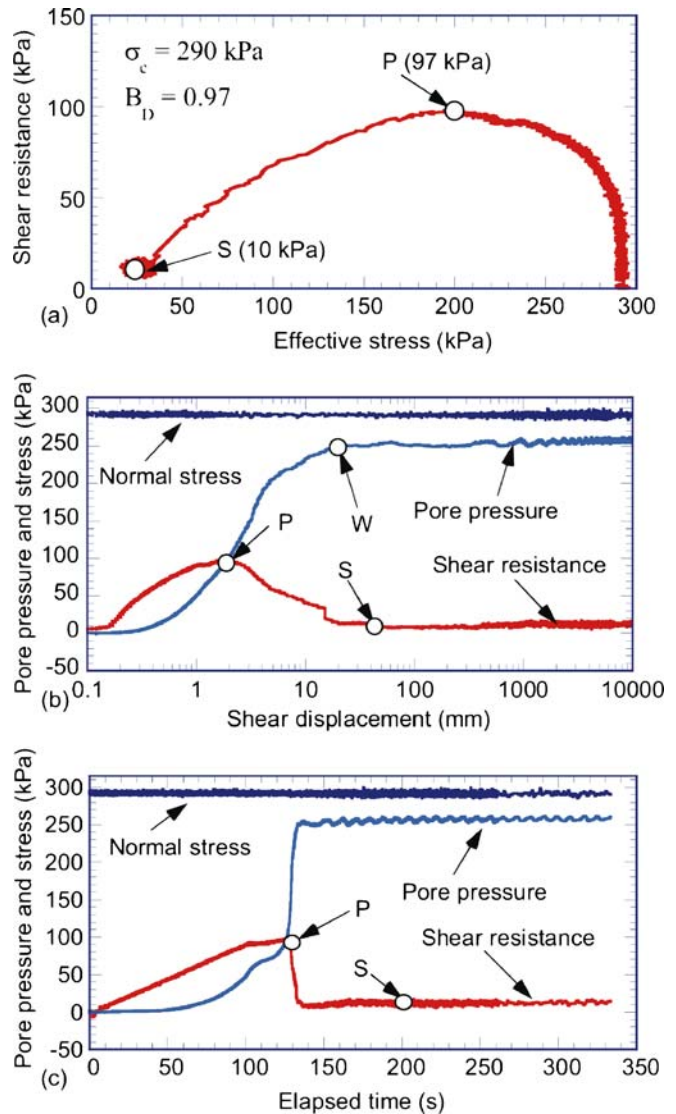


Fig. 10 Shear behavior of ING specimens (test 9) $D_r=31.5\%$, $\sigma_c=290$ kPa, $B_D=0.97$. **a** Stress path; **b** shear resistance, normal stress, and pore pressure vs displacement; **c** vs elapsed time

specimen exhibited a high brittleness index of 0.80. Careful examination of the pore pressure changes within the period under consideration may throw more light on the undrained response of WG specimens employed in this research. The sample mobilized its peak strength (P) at 1.77-mm displacement, at which point, pore pressure had risen to 60 kPa. Soon afterwards, the pore pressure rose further to 177 kPa (at point M in Fig. 11c), which amounted to a pore pressure ratio of 0.88, and remained constant until the experiment was terminated at 10 m. The sample is thought to have liquefied because of the high excess pore pressure built-up and the consequent low effective stress attained in the process.

Another specimen consolidated at about 250 kPa to a relative density of 29.5% displayed similar behavioral trend (Fig. 12). The instant the stress path reached the peak shear resistance at 80 kPa, the sample collapsed and the resultant excess pore pressure caused the shear resistance to drop rapidly until the steady state strength of about 13 kPa was reached. The brittleness index of the specimen was 0.83.

Another WG specimen consolidated at 290 kPa to a relative density of 29.5% (Fig. 13). The specimen mobilized a peak strength of 106 kPa and attained a steady-state strength of about 12 kPa, and in the process achieved a brittleness index of 0.88.

A drained test was undertaken to investigate the nature of volume changes associated with loose WG samples. Close examination of the test result (Fig. 14) of a sample consolidated at 196 kPa to $Dr=30.2\%$, shows that, soon after shearing commenced, the sample first suffered considerable volume reduction until about 30 mm, from which point the sample underwent little volume reduction until the test was terminated at 10 m.

Apparent collapse of the metastable structure might be essentially responsible for the excessive volume changes suffered until 30 mm in the drained test (Fig. 14), while grain crushing might account for the volume changes that followed.

Discussion

NAG, ING, and WG specimens at the same confining stress and similar relative densities responded to undrained loading in a

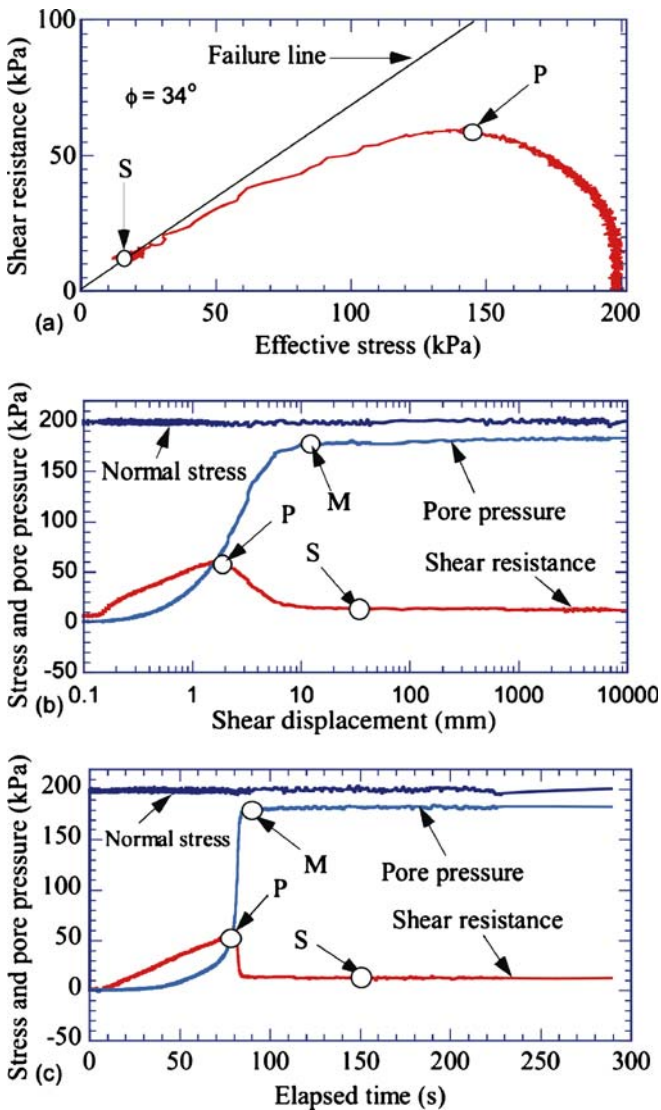


Fig. 11 Undrained response of WG specimen (test 10) with $Dr=29.5\%$, $\sigma_c=196$ kPa; $B_D=0.96$. a Stress path; b stress and pore pressure vs displacement; c vs elapsed time

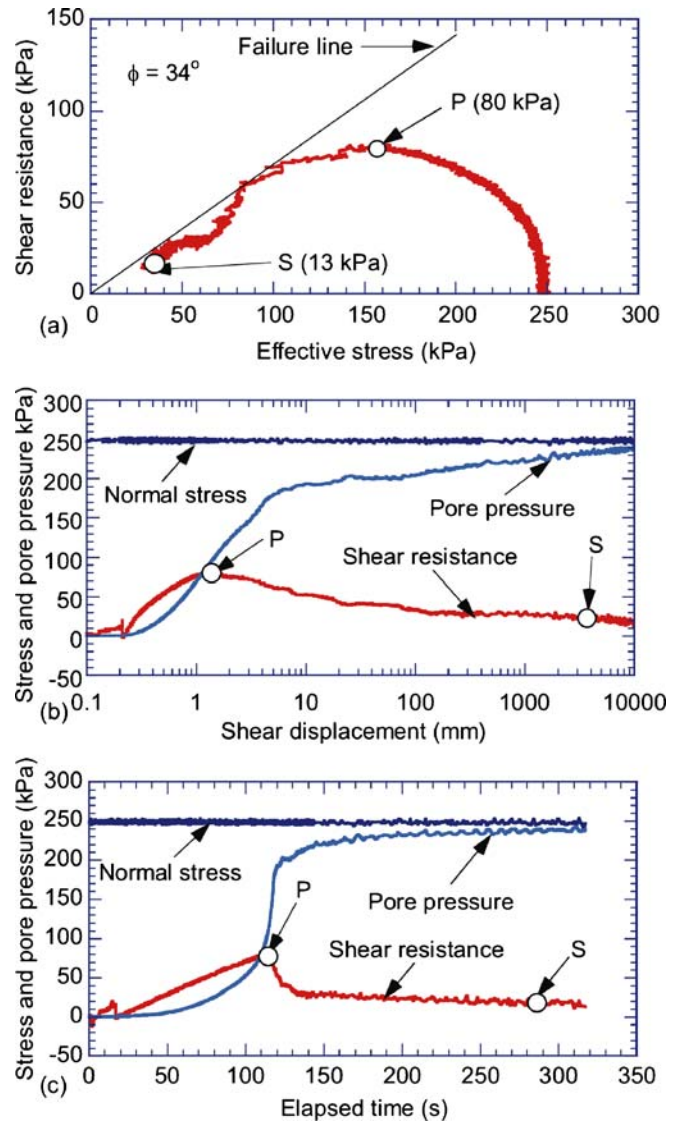


Fig. 12 Undrained response of WG specimens (test 11) $Dr=29.5\%$, $\sigma_c=250$ kPa, $B_D=0.96$. a Stress path; b shear resistance, normal stress, and pore pressure vs displacement; c vs elapsed time

purely contractive fashion. The failure pattern consisted of the attainment of peaks at small shear displacements, followed by rapid, continuous, and unidirectional loss of shear strength, until the samples reached their respective steady states without further changes in either shear resistance or effective stress during long deformation. This rapid reduction in strength has been attributed to the breakdown of a metastable structure and the consequent increase in pore pressure in the loose mass of soil. The results of the undrained tests presented indicate that tendency for volume reduction and the consequent increase in pore pressure in loose specimens are responsible for the considerable reduction in shear strength. Subjecting the specimens to long distances of shearing in the ring shear apparatus has helped clarify the effect of gradation, which, until now, has been poorly understood. To understand the nature and manner of volume changes occurring in loose specimens, drained tests on the same material at similar relative densities were conducted. Results of the tests (Figs. 3, 8, and 14) clearly show that loose specimens suffer considerable volume reductions. They also

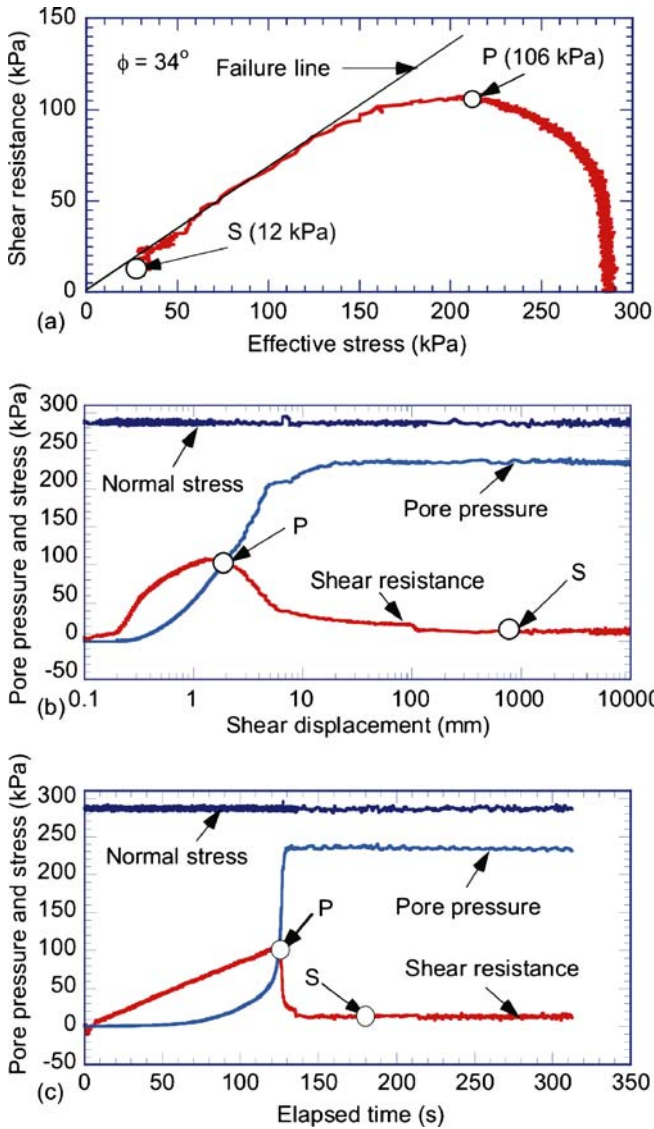


Fig. 13 Undrained response of WG specimens (test 12) $D_r=29.5\%$, $\sigma_c=290$ kPa, $B_D=0.96$. **a** Stress path; **b** shear resistance, normal stress, and pore pressure vs displacement; **c** vs elapsed time

indicate that the pore pressure generation in the undrained test might be associated with not only the collapse of metastable structure but also grain crushing. Because of the differences in relative density among the three kinds of specimens investigated in drained condition, a direct comparison of the drained results may answer little with regards to why the shear behaviors of these specimens differed significantly in undrained condition.

However, when the undrained stress paths of the three different specimens described are compared, there seems to be sufficient evidence suggesting that grading might have some effect on the shear behavior of NAG, ING, and WG specimens. It may be observed that the mechanisms of deformation in the NAG and ING specimens, especially close to the steady state, are different from those of the WG ones. The WG specimens, composed of a wide variety of grain sizes, tend to show greater peak and steady state strengths than the NAG and ING ones (Fig. 15). The results presented in Figs. 4, 7, and 11 show that at the same relative density and normal stresses of about 220 kPa for NAG, 202 kPa for ING,

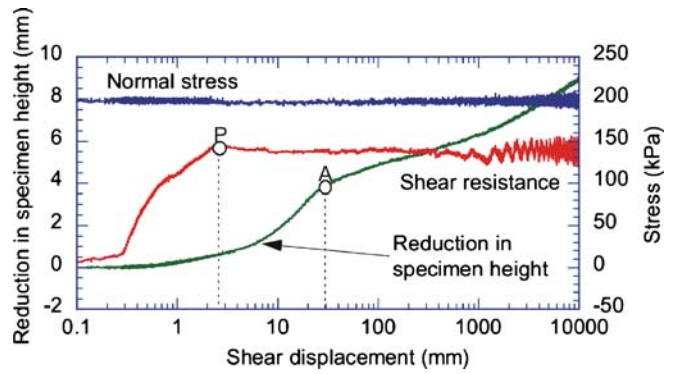


Fig. 14 Drained response of WG specimen (test 13) with $D_r=30.2\%$; $\sigma_c=196$ kPa; $B_D=0.96$

and 196 kPa for WG, the NAG, ING, and WG specimens attained respective peak strengths of 49, 54, and 60 kPa, while their respective steady states were 0, 5, and 12. Similarly, the results presented in Figs. 6, 9, and 12 show that, at almost the same relative density and normal stresses of about 260 kPa (for NAG and ING) and about 250 kPa (for WG), the NAG, ING, and WG specimens mobilized peak strengths of 70, 67, and 80 kPa, respectively, and achieved respective steady states of 0, 0, and 13 kPa. At higher normal stresses of about 290 kPa, the NAG, ING, and WG specimens achieved peak strengths of 85, 97, and 106 kPa, respectively, and attained respective steady state strengths of 0, 10, and 12 kPa (Figs. 5, 10, and 13).

Greater particle-to-particle contacts occasioned by the combination of a wide range of particle sizes in the WG specimens seem to be central to these higher values of strength observed. Stronger contacts between particles produce stronger resistance to shearing stress. Because one of the most important mechanisms in the deformation of granular materials is the relative sliding between particles, it seems reasonable that stronger contacts will resist such sliding better.

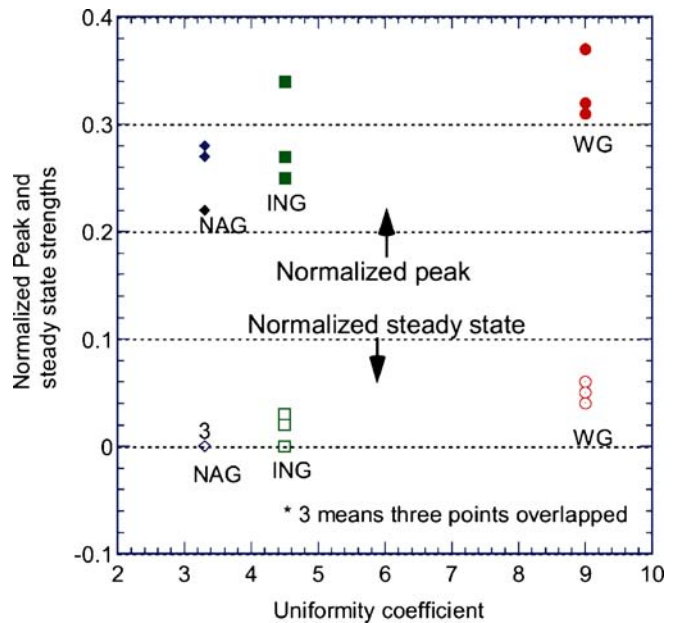


Fig. 15 Relationship between uniformity coefficient and normalized strengths of loose specimens

The relationship between uniformity coefficient and shear strengths normalized by the initial effective normal stress (consolidation stress, σ_c) is shown in Fig. 15. It may be seen that the higher the uniformity coefficient, the higher both the peak and the steady state strengths of the sands. The widely graded specimens have higher peak and steady-state strengths than the NAG ones. It may be important to note that the steady-state strengths of the NAG specimens were all nearly zero and, because of this, were plotted as a single point in Fig. 15.

Conclusions

A series of tests on sands with different particle gradations were undertaken to investigate their liquefaction potential when subjected to undrained shearing. On the basis of the result, the following conclusions are drawn:

1. Loose NAG, ING, and WG specimens at the same confining stress and relative density responded to undrained loading in a purely contractive fashion associated with the attainment of peaks at small shear displacement, followed by rapid, continuous, and unidirectional loss of shear strength until the attainment of low steady-state strength.
2. A relationship between uniformity coefficient and the shear strengths of the sands shows that the higher the uniformity coefficient, the higher both the peak and steady state strengths of the sands.
3. Because WG specimens have higher peak and steady-state strengths than the NAG ones, WG materials should offer greater resistance to liquefaction-inducing stresses than the NAG ones. NAG and ING specimens are much more likely to liquefy than WG ones when subjected to the same stress conditions.
4. The postfailure behavior of the NAG specimens below a relative density of 30% is significantly distinguished from those of the WG specimens in the sense that the NAG specimens underwent complete liquefaction. Complete liquefaction has been defined in this paper as the complete loss of shear strength after failure such that the steady strength is negligible.

References

Alarcon-Guzman A, Leonards GA, Chameau JL (1988) Undrained monotonic and cyclic strength of sands. *J Geotech Eng Div* 114(10):1089–1109

Bishop AW (1971) Shear strength parameters for undisturbed and remoulded soil specimens. *Stress-strain behavior of soils*. RHG Parry Ed, Cambridge University, Cambridge, UK, pp 3–58

Bishop AW (1973) Stability of spoil heap. *Q J Eng Geol* 6:335–376

Casagrande A (1936) Characteristics of cohesionless soils affecting the stability of slopes and earth fills. *J Boston Soc Civ Eng* 23(1):13–32

Casagrande A (1976) Liquefaction and cyclic mobility of sands: a critical review. *Harvard soil mechanics series*, no. 88. Harvard University, Cambridge, MA

Castro G (1969) Liquefaction of sands. Ph.D. thesis, Harvard University, Cambridge, MA

Castro G, Poulos SJ (1977) Factors affecting liquefaction and cyclic mobility. *J Geotech Eng Div* 103(GT6):501–516

Finn WDL, Bransby PL, Pickering DJ (1970) Effect of strain history on liquefaction of sands. *J Soil Mech Found Div* 97(SM6):1917–1934 (proceedings paper 7670)

Hardin BO, Drenevich VP (1972a) Shear modulus and damping in soils: design equations and curves. *J Soil Mech Found Div* 98(SM7):667–692 (proceedings paper 9006)

Hardin BO, Drenevich VP (1972b) Shear modulus and damping in soils: measurement and parameter effects. *J Soil Mech Found Div* 98(SM6):603–624 (proceedings paper 8977)

Herrera I (1964) *Dinamicos para Materiales y Estructuras del Tipo Masing*. *Bol Soc Mex Ing Sism* 3(1):1–8

Hutchinson B, Townsend D (1961) Some grading–density relationships for sands. *Proceedings, 5th international conference on soil mechanics and foundation engineering*, vol 1, pp 159–163

Kokusho T, Hara T, Hiraoka R (2004) Undrained shear strength of granular soils with different particle gradations. *J Geotech Geoenviron Eng* 130(6):621–629

Kondner RL, Zelasko JS (1963) A hyperbolic stress–strain formulation for sands. *Proceedings, 2nd Pan American conference on soil mechanics and foundation engineering*, pp 289–324

Konrad JM (1993) Undrained response of loosely compacted sands during monotonic and cyclic compression tests. *Geotechnique* 43(1):69–89

Kramer SL, Seed HB (1988) Initiation of soil liquefaction under static loading conditions. *J Geotech Eng* 114(4):412–430

Lade PV, Pradel D (1990) Instability and plastic flow of soils. *Experimental observations*. *J Eng Mech* 116(11):2500–2532

Negussey D, Wijewickreme WKD, Vaid YP (1988) Constant-volume friction angle of granular materials. *Can Geotech J* 25:50–55

Newmark NM, Rosenblueth E (1971) *Fundamentals of earthquake engineering*. Prentice-Hall, Englewood Cliffs, NJ, pp 162–163

Poulos SJ (1981) The steady state of deformation. *J Geotech Eng Div* 107(GT5):553–562

Poulos SJ, Castro G, France JW (1985) Liquefaction evaluation procedure. *J Geotech Eng Div* 111(6):772–792

Pyke RM (1973) Settlement and liquefaction of sands under multidirectional loading. Ph. D. thesis, University of California, Berkeley, CA

Sasitharan S, Robertson PK, Segoo DC, Morgenstern NR (1993) Collapse behavior of sand. *Can Geotech J* 30:569–577

Sasitharan S, Robertson PK, Segoo DC, Morgenstern NR (1994) State-boundary surface for very loose sand and its practical implications. *Can Geotech J* 31:321–334

Sassa K (1985) The mechanism of debris flow. In: *Proceedings of the 11th international conference on soil mechanics and foundation engineering*, San Francisco, CA, vol 3, pp 1173–1176

Sassa K (1988) Geotechnical model for the motion of landslides. *Special lecture of the 5th international symposium on landslides, 'landslides'*, vol 1. Balkema, Rotterdam, pp 37–55

Sassa K (2000) Mechanism of flows in granular soils. *Proceedings of the GeoEng2000, Melbourne*, vol 1, pp 1671–1702

Sassa K, Gonghui W, Fukuoka H (2003) Performing undrained shear test on saturated sands in a new intelligent type ring shear apparatus. *Geotech Testing J* 26(3):1–9

Seed HB, Idris IM (1971) Simplified procedures for evaluating soil liquefaction potential. *J Soil Mech Found Engr Am. Soc. Civ. Engrs*. GT3 109:458–482

Seed HB, Idriss IM (1969) Influence of soil conditions on ground motions during earthquakes. *J Soil Mech Found Div* 95(SM1):99–137 (proceedings paper 6347)

Sladen JA, D'Hollander RD, Krahn J (1985) The liquefaction of sands, a collapse surface approach. *Can Geotech J* 22:564–578

Vaid YP, Chern JC (1985) Cyclic and monotonic undrained response of saturated sands. *Advances in the art of testing soils under cyclic conditions*. American Society of Civil Engineers Convention, Detroit, MI, pp 120–147

Vaid YP, Fisher JM, Kuerbis RH, Negussey D (1990) Particle gradation and liquefaction. *J Geotech Eng* 116(4):698–703

Vasquez-Herrera A, Dobry R, Ng TT (1988) Pore pressure build-up and liquefaction failure of anisotropically consolidated sand due to cyclic straining. *Proceedings of conference on hydraulic fill structures*, Fort Collins. American Society of Engineers, New York, pp 346–366

Wafid MA, Sassa K, Fukuoka H, Wang G (2004) Evolution of shear-zone in undrained ring shear tests. *Landslides J Int Consort Landslides* 1:101–112

Wang G, Sassa K (2001) Factor affecting the rainfall-induced flowslides in laboratory flume tests. *Geotechnique* 51(7):587–599

Wang G, Sassa K (2002) Post-failure mobility of saturated sands in undrained load-controlled ring shear tests. *Can Geotech J* 39:821–837

Yamamuro JA, Lade PV (1999) Experiments and modeling of silty sands susceptible to static liquefaction. *Mech Cohes-Frict Mater* 4(6):545–564

Yoshimine M, Robertson PK, Wride CE (1999) Undrained shear strength of clean sands to trigger flow liquefaction. *Can Geotech J* 36:891–906

O. Igwe · K. Sassa · F. Wang

Research Centre on Landslides, Disaster Prevention Research Institute, Kyoto University, Kyoto, Japan

e-mail: igwe@landslide.dpri.kyoto-u.ac.jp